Experimental Investigation of a Hall Thruster Internal Magnetic Field Topography*†

Peter Y. Peterson‡, Alec D. Gallimore§, and James M. Haas**
Plasmadynamics and Electric Propulsion Laboratory
Department of Aerospace Engineering
The University of Michigan
College of Engineering
Ann Arbor, MI 48109 USA
Phone: 734-764-4199
Fax: 734-763-7158
pypeters@engin.umich.edu

IEPC-01-030

Magnetic field measurements were made in the discharge channel of the 5-kW-class P5 laboratory-model Hall thruster to investigate what effect the Hall current has on the static, applied magnetic field topology. The P5 was operated at 1.6 kW and 3.0 kW with a discharge voltage of 300 V. A miniature inductive loop probe (B-Dot probe) was employed to measure the radial magnetic field profile inside the discharge channel of the P5 with and without the plasma discharge. These measurements are accomplished with minimum disturbance to thruster operation with the High-speed Axial Reciprocating Probe (HARP) system. Data are presented at axial locations ranging from 1 cm downstream of the anode to 6 cm downstream of the thruster exit plane, and at several radial positions covering the width of the discharge chamber. The results of the B-Dot probe's measurements indicate a change in the magnetic field topography, from that of the vacuum field measurements. The measured magnetic field profiles are then examined to determine the possible nature and source of the difference in the vacuum and plasma magnetic field profiles in the discharge chamber of the P5 thruster.

Introduction

The requirements of a spacecraft propulsion system for new mission profiles have increased recently beyond the current level of existing technology. An example of one recently prescribed requirement is for a propulsion system to operate in "dual-mode". Dual-mode is the ability of a thruster to operate efficiently in both a high-thrust and low-specific impulse (e.g., for orbit transfer operations) mode and a high-specific impulse and low-thrust mode (e.g., for station-keeping) [1,2]. Other design drivers for advanced space propulsion systems revolve around human space exploration. A piloted mission to Mars for example would require a reliable propulsion system with high power, high performance, and long life.

A favorable candidate for these types of missions is the closed-drift Hall thruster. A Hall thruster is a coaxial plasma device in which an applied magnetic field effectively traps electrons in the discharge channel of the thruster. The electrons are usually emitted from an external cathode while a magnetic circuit composed of electromagnetic solenoids and pole pieces typically creates the applied magnetic field. The magnetic circuit of a typical Hall thruster produces a radial magnetic field topology at the exit of the discharge channel with peak fields on the order of a few hundred-gauss. If the magnetic field topology in the discharge channel is designed properly, the accelerating ions will experience a focusing effect through what is referred to as a magnetic lens [3].

* Presented as Paper IEPC-01-030 at the 27th International Electric Propulsion Conference, Pasadena, CA, 15-19 October 2001.
† Copyright © 2001 by Peter Y Peterson. Published by the Electric Rocket Propulsion Society with permission.
‡ Graduate Student, Aerospace Engineering.
§ Associate Professor, Aerospace Engineering and Applied Physics.
** Former Graduate Student, Aerospace Engineering, Currently a Research Scientist at Edwards Air Force Base

One of the main characteristics of a Hall thruster is the azimuthally drifting electrons. These electrons form a region of azimuthal current in the discharge channel that is typically on the order of 5-10 times the discharge current. This estimate is based on Hall parameters expected in Hall thruster discharge chambers; e.g., 200-300 [4]. This estimate can lead to Hall currents on the order of 150 A for a 5 kW Hall thruster.

Recent plasma measurements inside the discharge channel of the P5 indicate that the true, effective Hall parameter ranges from 10-20 near the anode to approximately 1000 in the acceleration region [5,6]. These results suggest that the Hall current may be larger than previously thought, and that its induced magnetic field could impact the applied magnetic field topology significantly. As the magnitude of the Hall current increases at higher thruster power levels, the effects of the self-magnetic field induced by the Hall current may become important. As the self-magnetic field magnitude increases, its effect on the magnetic circuit applied field topology is greater, thus decreasing the chances of maintaining the desired magnetic lens profile in the discharge channel. In designing next-generation Hall thrusters, the magnetic field topology for a given magnetic circuit design can be predicted with great precision by using 3-D magnetostatic computer codes. However, to accurately predict the magnetic field topology during thruster operation, a better understanding of the effects of the magnetic field induced by the Hall current is needed.

The University of Michigan Plasmadynamics and Electric Propulsion Laboratory (PEPL) has endeavored in the past to develop and improve plasma diagnostic techniques to be used on plasma propulsion systems [7-14]. An attempt to map the magnetic field topology near the exit of a D-55 Anode Layer Thruster (TAL) was performed at PEPL [14]. However, these measurements were limited to 15 mm downstream of the exit plane due to the large perturbations in thruster discharge current that ensued when the Hall probe was placed closer to the engine. It was concluded that the Hall probe was entering the Hall current region and thus disrupting the stable operation of the thruster. To continue the research effort initiated by the D-55 very-near-field investigation, and to gather knowledge on the effects of the self-induced magnetic field at high power operation of a Stationary Plasma Thruster (SPT), a miniature inductive loop probe (B-Dot probe) system was developed and used in conjunction with the PEPL High-speed Axial Reciprocating Probe (HARP) system to map the radial magnetic field of the P5 Hall thruster.

The University of Michigan's HARP system was designed to address concerns associated with placing probes within an operating Hall thruster. These concerns include probe life and thruster perturbation. These concerns are addressed by the high sweeping speed of the HARP system (described below). The HARP system also provides a unique opportunity to incorporate a time response B-Dot probe by virtue of its motion. B-Dot probes are typically used for pulsed and inductive plasma discharges with time-varying magnetic fields [15-17]. However, by combining the high speed of the HARP table (dx/dt) with the B-Dot probe response to a time-varying magnetic field (dB/dt), one can measure a change in a magnetic field magnitude (dB/dx) as the probe is swept into the discharge channel of the thruster.

The B-Dot probe, as a plasma diagnostic device, has been used in the past to measure the properties of a Hall thruster. Barkalov incorporated two inductive loops into a pulsed Hall thruster to measure the location and magnitude of the Hall current [18]. The two coils were located along the inner and outer walls of the ceramic discharge channel. The Hall current was determined to be a maximum of approximately 30 A, for a 300 V 15 A plasma discharge. The Hall thruster investigated in this reference had outer diameter of 160 mm, a width of 30 mm, and a depth of 60 mm.

This paper will briefly describe the experimental facilities, the Hall thruster, and the HARP system. The theory of inductive loop operation is reviewed, as are the construction, set-up, and calibration of the B-Dot system. The thruster magnetic field profiles both in vacuum and in the presence of the plasma discharge are presented and discussed. Finally, several avenues are investigated to examine the nature of the observed change in the magnetic field profiles between the vacuum and plasma conditions.

Experimental Apparatus

Vacuum Facilities

All the experiments were conducted in the University of Michigan's Large Vacuum Test Facility (LVTF) that has a diameter of 6 meters and a length of 9 meters. Two 2,000 CFM blowers and four 400 CFM mechanical pumps evacuate the LVTF chamber to moderate vacuum (30 - 100 mTorr). To reach high vacuum the LVTF is equipped with seven CVI TM-1200 cryopumps, with a combined pumping speed of ~500,000 l/s on air, and ~240,000 l/s on xenon. The cryopump system can be operated with any number of pumps in use. For the experiments reported here the LVTF was operated with only four cryopumps to match operating conditions of prior experiments [5,19]. At the four-cryopump configuration, the combined pumping speed of 140,000 l/s on xenon with a base pressure 1.6×10^{-7} Torr was achieved. At a 10.2 mg/s anode mass flow and a 0.6 mg/s cathode mass flow the operating pressure of the LVTF was 1.1×10^{-5} Torr (xenon).

The schematic of the LVTF is shown in Fig. 1. The Hall thruster was mounted in the center of the vacuum chamber on a X-Y computer-controlled linear positioning system.

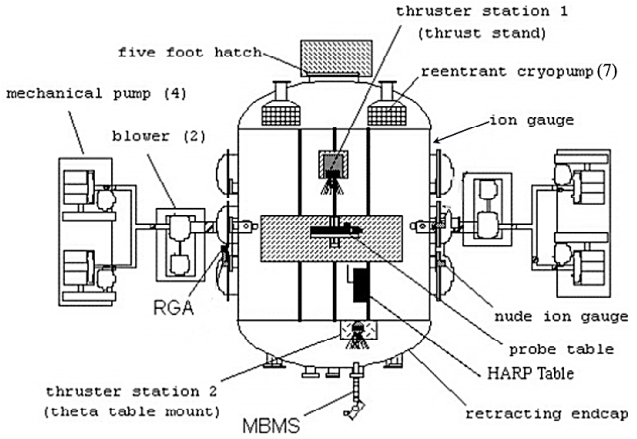

Figure 1, Schematic of the LVTF.

Hall Thruster

The experimental results presented in this paper were conducted on the 5-kW-class laboratory model P5 Hall thruster. The P5 Hall thruster was developed by the University of Michigan and the Air Force Research Laboratory to serve as a test-bed for new diagnostics and for investigating Hall thruster processes. Depicted in Fig. 2, the P5 has an outer diameter of 170 mm, a channel width of 25 mm, and a channel depth of 38 mm.

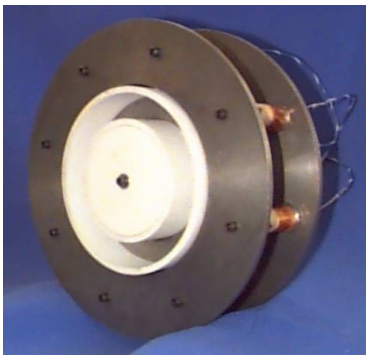

Figure 2, P5, 5 kW class laboratory model Hall thruster.

The P5 performance characteristics, presented in a previous work [20], are comparable to commercially available 5 kW thrusters. Table 1 shows the measured performance characteristics of the P5 for the two operating conditions used in this experiment. The hollow cathode used for this test was provided by Moscow Aviation Institute (MAI). The cathode provides thermally emitted electrons to the discharge by a small disk of lanthanum hexaboride (LaB_6).

Table 1, P5 thruster performance ranges for the experiments discussed in this work [18].

Case	Vd [V]	Id [A]	Power [kW]	Total Specific Impulse [sec]	Total Efficiency
(1)	300	5.4	1.6	1550	48%
(2)	300	10.1	3.0	1650	51%

High-speed Axial Reciprocating Probe

The HARP system consists of a LM1210 high-speed linear motor and encoder manufactured by Trilogy. The linear encoder provided a linear resolution of 5 microns to a Pacific Scientific SC950 digital brushless servo drive controller. A computer controls the position, speed, acceleration, deceleration, and sweep configuration for the HARP system. The linear table

was placed within a stainless steel shroud encased with graphite plates (Figs. 3 and 4).

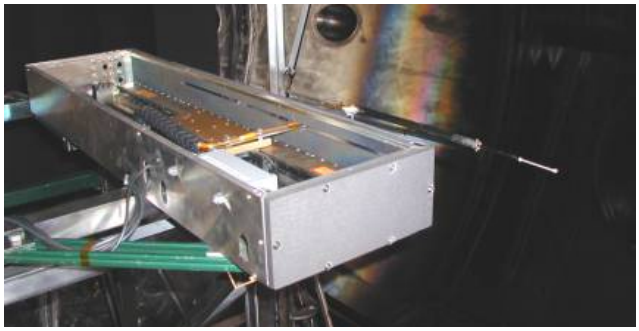

Figure 3, PEPL's High-speed Axial Reciprocating Probe (HARP) system. The top cover of the shroud has been removed to show the linear motor and B-Dot integrator.

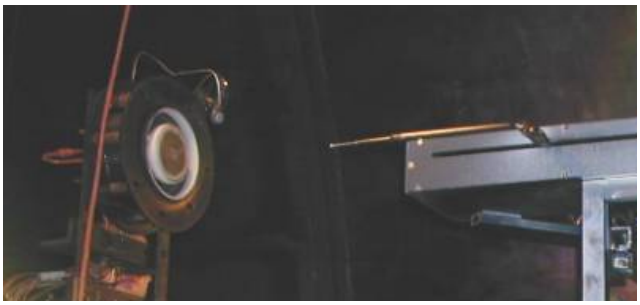

Figure 4, Typical configuration of the HARP table and the P5 thruster. The picture shows the B-Dot probe in its zero position, which is 150 mm downstream of the thruster exit plane. A sweep of the probe occurs over 180 mm.

The primary issue involving internal probe measurements of a Hall thruster is the ability of the probe to survive in the presence of the discharge plasma and Hall current. Ablation of probe material also affects thruster operation. Therefore, the main driving factor in determining the maximum resonance time that a probe can remain in the discharge channel of a thruster is the characteristic time for probe material ablation. The ablation time for 99%-pure alumina has been determined to be approximately 150 ms for a 5 kW plasma discharge [5]. The time that the B-Dot probe spent in the discharge channel for these experiments was approximately 80 ms ±10 ms. The peak velocity and acceleration of the HARP for these experiments was approximately ±5.5 m/s and 130 to -100 m/s^2, respectively.

Another important issue is the actual heating of the probe during the sweep into discharge plasma. If the probe resonance time in the discharge plasma is significantly long to allow the probe heat up, thus changing the electrical characteristics of the probe's circuit, the results of the mapped magnetic field profile for the plasma case may differ from that of the vacuum measurements. Employing the same method for the determining the ablation time of a material in a 5 kW plasma discharge [5], one can determine a bulk heating of a probe of a given size, material, discharge plasma parameters, and exposure time. It was determined analytically that the maximum increase in temperature for a typical ceramic probe used during this investigation will be approximately 1.5 degrees per sweep.

Inductive Loop Probe

To measure the internal magnetic field topography of an operating Hall thruster, there were two methods that were considered. The first method was a Hall probe, and the second was an inductive loop probe. Four criteria were established to determining the practicality of both methods. The four criteria were size, thermal response, fabrication issues, and cost. The size of the magnetic field probes that could be constructed from each method was comparable. The thermal response of each of the potential methods should not be a factor due the duration that a probe would spend in the plasma discharge, as discussed in the description of the HARP positioning system. The fabrication of a Hall probe system would have been less complex in assembly than the winding of the inductive coil for the B-Dot system. The cost of the miniature magnetic field probe was the deciding factor in choosing which probe system would be used for this investigation. Due to the nature of the HARP system and the size of the discharge channel of the P5 thruster, there was always the possibility that the probe would come into contact with the thruster's channel walls or the anode itself, due to small misalignments of the thruster. Considering the cost of miniature Hall probes, this avenue of mapping the magnetic field of the discharge channel was turned down in favor of the B-Dot system.

The inductive loop probe is a well-established plasma diagnostic technique for time-varying magnetic fields. Typical plasma discharges that make use of the B-Dot

probing technique include pulsed and inductive plasmas [15-17]. The basic operating principle of the B-Dot probe is based on the observation that current is induced in a conducting coil immersed within a time-varying magnetic field. The ensuing output voltage from the coil is proportional to its cross-sectional area (A), the number of turns in the coil (N), and the time characteristic of the magnetic field (dB/dt). The expression of the voltage output from a B-Dot probe is given as Eq. (1).

$$V = nA\,dB/dt \tag{1}$$

Since Hall thrusters typically operate with a steady applied magnetic field, direct application of the B-Dot probe is problematic. To circumvent this issue, the HARP position system was used to provide a time-varying magnetic field signal by virtue of moving the probe into (and out of) the applied, steady magnetic field. Therefore, by combining the motion of a high-speed table (dx/dt) with the integrated signal of a B-Dot probe in a time-varying magnetic field (dB/dt), one is able to measure the DC applied magnetic field as the probe is swept into and out of the Hall thruster discharge channel.

A dual-supply integrator that incorporates an Analog Devices AD549 ultra-low input bias current operational amplifier and a AD624 precision instrumentation amplifier was chosen to integrate the B-Dot probe raw signal. The expression of the integrated output voltage from a B-Dot probe is shown in Eq. (2)

$$V = \frac{nA}{RCG} B \tag{2}$$

Where the G is the amplifier gain, RC is the integrators resistor and capacitor, respectively, and B is the measured magnetic field. The amplified voltage output from the B-Dot probe integrator circuit was recorded with a Tektronix TDS 540 digital oscilloscope in high-resolution acquisition mode. The data were then downloaded to a computer for processing. A diagram of the integrator circuit used in the experiments described in this paper is shown in Fig. 5.

The B-Dot probe support structures used for this investigation were constructed of 99% alumina ceramic tubes and ceramic paste. The inductive loops were wound with 38 and 40 gauge magnetic wire with enamel nonconductor coatings. The coils used in this investigation were wound around 1.6 to 2.5 mm diameter alumina ceramic tubes 2.2 to 2.5 mm in length. The number of turns in the probe coils ranged from 89 to 136. The final dimensions of the B-Dot probes used in this investigation ranged from 4 to 4.3 mm in diameter and 4 to 4.2 mm in length.

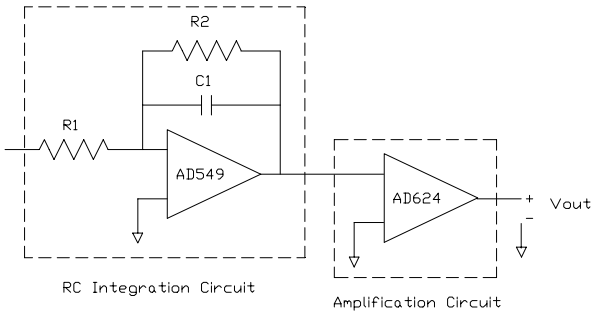

Figure 5, B-Dot Integrator and Amplifier circuit. Where R1 and C1 are the primary integration components.

Figure 6 shows the mapped area inside the discharge channel of the P5 thruster. The B-Dot probe was axially swept from 150 mm downstream of the exit plane to 10 mm in downstream of the anode. This axial sweep profile was repeated for three radial positions, 3.81 mm from the inner wall, the centerline (at 12.7 mm), and 3.81 mm from the outer wall of the discharge channel. In an attempt to minimize the heating of B-Dot probe between sweeps, the probe home position was set to 152 mm downstream of the thruster exit plane. The cathode plane was located 50 mm downstream of the thruster exit plane and was oriented 45° counter-clock wise from the plane mapped. The results presented in this paper will cover the first 100 mm downstream of the anode.

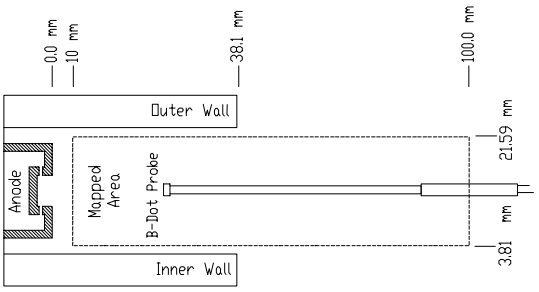

Figure 6, B-Dot probes mapped area inside and outside of the P5 discharge channel.

Results and Analysis

Calibration of B-Dot Probe

The initial goal of this experiment was to calibrate the B-Dot probe and integrator circuit with an electric and magnetic field (ExB) source. The idea behind the ExB source was to approximate, under a controlled and understood manner, the fields that the B-Dot probe would experience when the probe is traveling through the discharge channel of an operating thruster. The ExB source was comprised of two electromagnetic coils, to provide the magnetic field, and two parallel plates for the electric field. The configuration of the ExB source can be seen in Fig. 7.

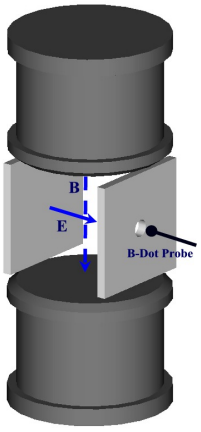

Figure 7, The ExB source configuration.

The magnetic field of the ExB source was first mapped using a NIST-traceable Walker Scientific MG-5DAR Hall probe. Then the B-Dot probe and HARP systems were configured to measure the ExB source with either the applied magnetic and/or static or time varying electric fields. A time varying electric field was simulated to approximate the oscillations of the discharge plasma in a Hall thruster during normal operation. All parameters of the B-Dot probe and HARP, such as speed, acceleration, deceleration, probe sweep length, and transmission line length that would be used during experiments with the P5 were used in the calibration runs.

A Kikusui power supply provided a constant current of 9 A to the ExB source to drive a 167 Gauss traverse magnetic field in the center of the ExB source. A Kepco Bipolar power supply and WaveTek frequency generator was used to apply a 15 kV/m static or time varying (11 kHz) electric field across the plates that were used to drive the electric field. This electric field magnitude was chosen to represent the typical value expected in 300 V Hall thruster discharge chambers. However, the peak electric field, which resides in a small region of the discharge chamber at the onset of the acceleration zone, can reach 25 kV/m at 300 volts and 5.4 A, and 20 kV/m at 300 volts and 10 A according to the internal emissive probe measurements [5,19]. The 15 kV/m that was used during the calibration of the B-Dot probes should still indicate if the B-Dot probes are influenced by the presence of a steep electric field.

Figure 8 shows the measured magnetic field profile of the ExB source as measured by the B-Dot probe with and without an applied electric field. Figure 9 presents the same measurements in the presence of an applied static or time varying (11 kHz) electric field of 15 kV/m. The measured data presented in Figs. 8 and 9 are composed of five sets of B-Dot traces averaged together at the same ExB source input settings. Figures 8 and 9 also contain the Hall probe traces of the ExB source at the two investigated conditions.

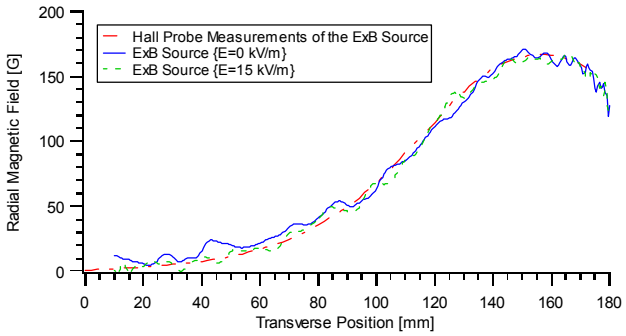

Figure 8, B-Dot and Hall probe measurements of the ExB source {I _Coil = 9 A}.

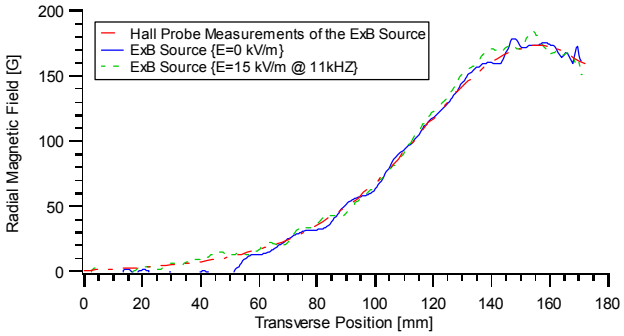

Figure 9, B-Dot and Hall probe measurements of the ExB source with an applied oscillating electric field {I _Coil = 9 A}.

As can be seen in Figs. 8 and 9 the B-Dot probe captured the profile and magnitude of the ExB source. The presence of the 15 kV/m static and time varying electric field had no noticeable effect on the measured magnetic field from the B-Dot probe.

Vacuum Field Measurements with B-Dot Probe

The vacuum magnetic field profiles of the P5 thruster were mapped using the B-Dot and HARP systems along the radial and axial positions described earlier. Two thruster power levels were investigated; 1.6 kW and 3.0 kW, both at a discharge voltage of 300 V. The inner and outer electromagnet coils were operated in a manner that minimized the discharge current of the thruster. Once these coil currents were determined for both power levels, the P5 discharge was extinguished while the magnets were left on for vacuum field measurements.

The B-Dot and Hall probe vacuum field measurements of the P5 at coil current settings for 1.6 kW and 3.0 kW are shown in Figs 10 and 11, respectively. The thruster exit plane and the mid-plane of the magnetic circuit outer and inner front poles are labeled in these figures. Once again, each B-Dot profile presented represents the average of 5 or more data sweeps. All trends observed in individual B-Dot sweeps are captured in the average profile.

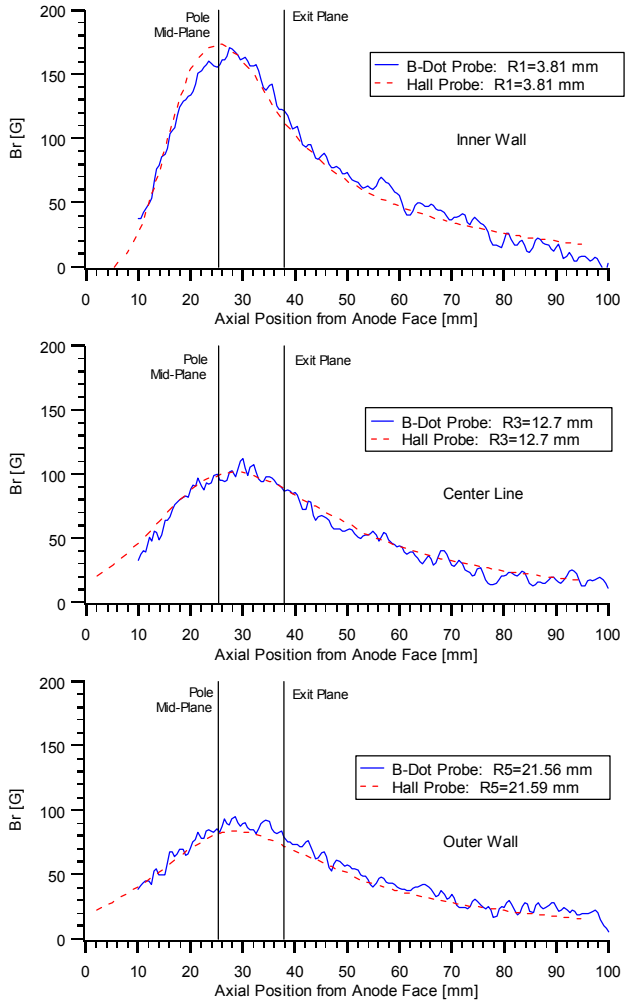

Figure 10, Vacuum magnetic field profiles of the P5 at 1.6 kW {I_in = 2 A, I_out = 1 A}

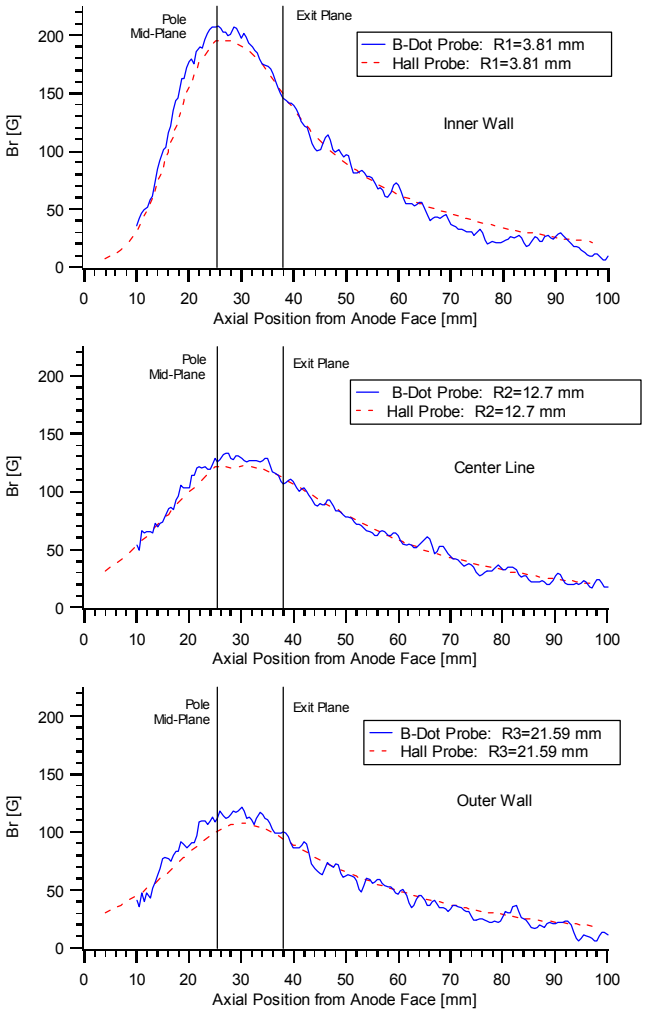

Figure 11, Vacuum magnetic field profile of the P5 at 3.0 kW {I_in = 3 A, I_out = 2 A}

The figures show that magnetic field profiles measured with the B-Dot probe match those of the NIST-traceable Hall probe for both coil settings.

Magnetic Field Measurements with Discharge

The discharge channel radial magnetic field with the P5 thruster operating at 1.6 kW and 3.0 kW was mapped at three radial positions. The P5 was operated for a minimum of forty minutes before B-Dot sweeps were made to allow the engine to reach thermal equilibrium. Thermal equilibrium was reached when the electromagnetic coils voltages of the magnetic circuit would stabilize. This step was conducted to ensure that any anomalies measured with the B-Dot probe were not due to thermal expansion of the magnetic circuit components throughout the duration of the experiment. The results of the B-Dot probe sweeps for the 1.6 kW thruster power level (300 volt, 5.4 A) are shown in Fig. 12. Figure 12 also contains a plot of the thruster discharge current as a function of probe position and the corresponding vacuum Hall probe magnetic field measurements.

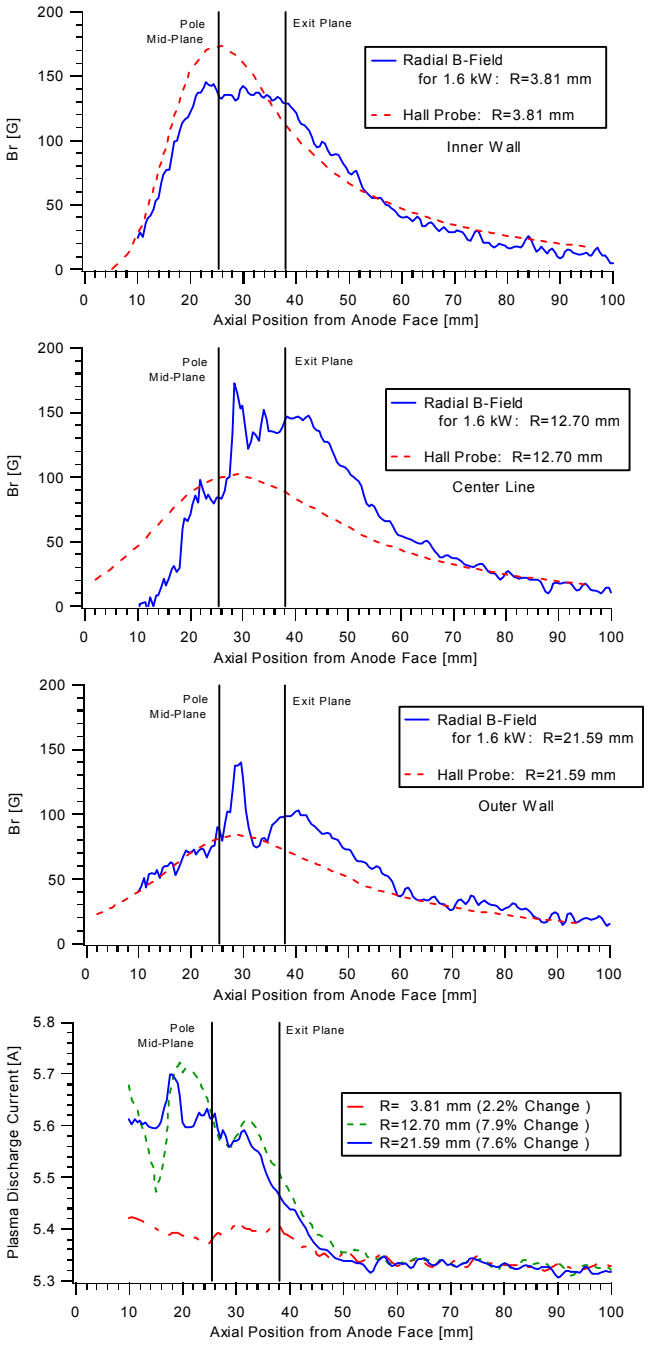

Figure 12, B-Dot probe magnetic field data at 1.6 kW and thruster discharge current as a function of probe position.

As can be seen in Fig. 12, the magnitude and profile of the magnetic field in the discharge channel of the P5 Hall thruster is affected by the presence of the plasma discharge.

B-Dot probe, vacuum Hall probe, and thruster discharge current data for the 3.0 kW power level are shown in Fig. 13.

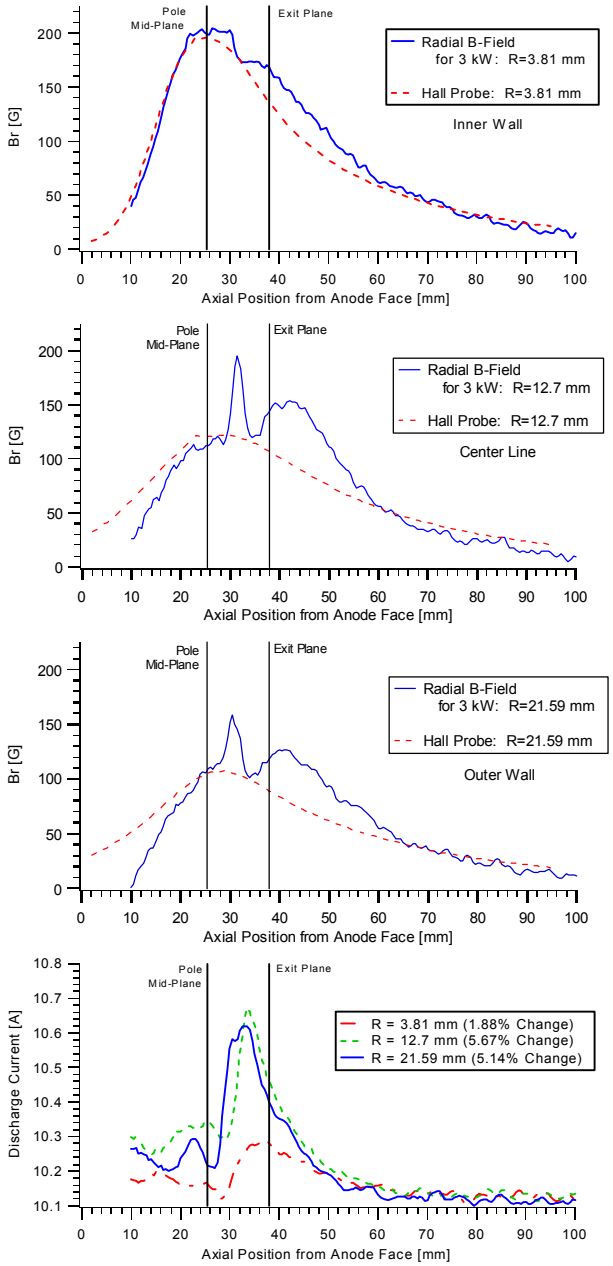

Figure 13, B-Dot probe magnetic field data at 3.0 kW and thruster discharge current as a function of probe position.

Once again the B-Dot profiles with the thruster operating at 3.0 kW differ from those in vacuum at the identical magnet settings. There are several possible explanations to account for these measured differences in the magnetic field profiles. The first and foremost explanation, assuming that the B-Dot probe is functioning properly, is the effect of the azimuthal electron drift (Hall current) self magnetic field. As discussed earlier, the Hall current of a closed-drift thruster can be 5 to 10 times the discharge current [4] or in light of recent internal plasma parameter measurements [5], possibly much higher.

In both the 1.6 kW and 3.0 kW cases we see that the B-Dot probe magnetic field profiles with the discharge plasma, closely match the vacuum field profiles along the inner wall of the discharge channel. However, the profiles are significantly different near the outer wall of the discharge channel and particularly along the center of the channel.

The largest differences in profiles occur slightly downstream of the thruster exit plane. In the 1.6 kW results, there is a spike in the measured magnetic field 10 mm inside of the discharge channel. A characteristic spike exists in the 3.0 kW data as well, however in this case the spike is 7 mm inside the thruster channel. Neither of these spikes nor the large increases in the B-Dot magnetic field profiles corresponds to locations of peak electric fields in the thruster [5]. The peak electric fields of the P5 are located approximately 5 mm inside the discharge channel for the 1.6 kW thruster power level and approximately 2 mm inside the channel for the 3.0 kW power level [19] (data not shown).

Thruster discharge current was recorded as the probe entered the discharge channel (Figs. 12 and 13). The maximum disturbance to the thruster discharge current was 8%; during the centerline sweep at the 1.6 kW power level. The axial region where the greatest perturbation in the thruster discharge current was recorded corresponds to a drop in the measured magnetic field profiles for each of the three radial sweeps for the 3.0 kW test condition. This can also be seen in the outer wall sweep of the 1.6 kW case. A possible explanation for these features is that the probe is blocking the natural path of the Hall current in the thruster channel. This explanation can also be argued by the greater perturbation to the thruster

discharge current for the centerline and outer wall sweeps. This area of the discharge channel is believed to be the location of the majority of the Hall current for the P5 thruster [5].

Another possible explanation that is less likely is thermal expansion of the magnetic circuit. However, this prospect was investigated by measuring the vacuum field profiles of the thruster before and immediately after the thruster was operated for an extended amount of time. No discernable changes in the vacuum field profiles were observed during the analysis of the data (not shown).

One final possibility for the measured difference in the results from the vacuum and plasma discharge profiles is that the B-Dot probe output voltage is perturbed by the high electric field in the discharge channel of the thruster. Several precautions were addressed during the fabrication and calibration of the B-dot probe system. The first was to place the integrator circuit as near as possible to the probe, which meant that the integrator was located in the shroud that covers the HARP table (Fig. 3). There was no indication, from the baseline sweeps of the HARP table and the B-Dot system, of electrostatic interference in the probe or the circuit from the operation of the HARP table alone. Another precaution addressed was to add a low resistance to the output of the B-Dot probe through the selection of the transmission lines and circuit design, thus effectively providing the B-Dot probe with a voltage divider for any unavoidable electrostatic pickup [15]. The final precaution was to calibrate the B-Dot system with an ExB source as described earlier. It was shown in Fig. 10 that as the B-Dot probe swept the ExB source with a known applied magnetic and static or time varying electric fields that there was no indication of the probe being affected by the presence of a large electric field.

Discussion

To understand the data presented in this paper several avenues were investigated. The first approach was to make use of recent Hall parameters calculations inside the discharge chamber of a Hall thruster [5,6], which determined that the Hall parameter could be as high as 1000 at the exit of the discharge channel. The Hall parameter is defined as the ratio between the azimuthal electron current (Hall current) and transverse (axial) electron current as seen in the following expression.

$$\Omega = \frac{j_{Hall}}{j_{ez}} = \frac{I_{Hall}}{I_{ez}} \frac{A_{ez}}{A_{Hall}} \qquad (3)$$

The axial electron current ranges from 25 to 30 percent of the discharge current [21]. Assuming the majority of the Hall current resides in a region near the exit of the discharge channel and encompasses the width of the channel and given a Hall parameter of 1000, we find that the Hall current is on the order of 90 A. A simple calculation for a self magnetic field, induced by the Hall current, can be made using Biot-Savart law for a current flowing in a long straight wire.

$$B = \frac{\mu_0 I_{Hall}}{2\pi R} \qquad (4)$$

This first order calculation yields an induced self-field of approximately 15 Gauss 7 mm downstream of the center of the prescribed Hall current region.

The first order calculation of the self-field does not express the overall mechanism of the induced magnetic field profile in a Hall thruster. The Hall thruster applied magnetic field topography is a consequence of the design of the system's magnetic circuit. It is known that changing one component of the magnetic circuit; e.g. screen length, thickness, or width, could lead to considerable modification to the magnetic field topography in the channel of a thruster [22]. As well, introducing a magnetic field source in the center of the discharge channel may alter the magnetic field structure. To address the concerns of a self-field influence on the applied magnetic field, a 3D magnetostatic simulation using Magnet6 by Infolytica was done. Figure 14 is an illustration of the 3D model used in the simulation.

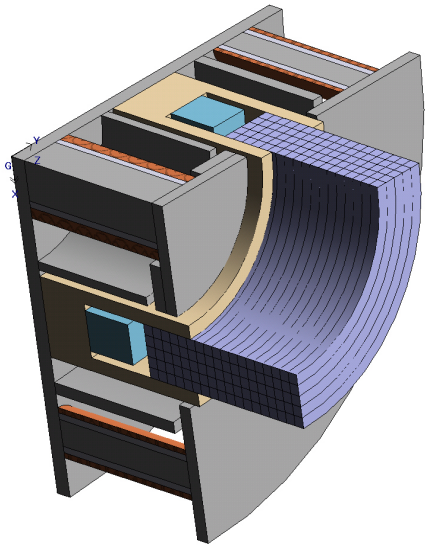

Figure 14, The 3D quarter model used in Magnet6 to simulate P5 self-field.

The model of the P5 Hall thruster, presented in Fig. 14, was setup to simulated the influence that the Hall current self-field has on the applied magnetic field from the region 10 to 100 mm downstream of the anode. The area of investigation continues past the exit of the discharge channel since it has been shown that a good portion of the ion acceleration occurs past the thruster's exit [5,23]. Therefore, this region should be investigated as another source of self-field for the thruster. The 3D model also takes into account the influence of all the self-fields from each Hall current regions on a single point of interest. The Hall current for this simulation was determined in the similar manner as in the first order calculation above, except five sets of Hall parameter data across the channel width and ranging from 10 to 100 mm downstream of the anode were used. To reduce computational time and model complexity the calculated Hall current profiles were interpolated to 90 regions, approximately 5 mm by 5 mm each, as seen in Fig. 14. The sum current for all the Hall current regions inside and outside of the discharge channel equated to a total Hall current of 156 A, which is greatly different than the predicted 27 to 54 amps for P5 operating at 5.4 A [4]. The ratio of the Hall to the discharge currents for the calculated Hall current above is $I_{Hall}/Id = 28.8$. This ratio would indicate an average Hall parameter for the P5 thruster, for the 90 regions method, of approximately 478 ($\Omega \approx 478$). The main difference in the Hall parameter for the P5, as compared to the value given by Kim [4], is that the calculation of the P5 is accounting for the ion acceleration that occurs downstream of the exit plane. Figure 15 illustrates the axial profiles of the calculated Hall current for five radial sweeps across the discharge channel and the sum of the Hall current as a function of axial position.

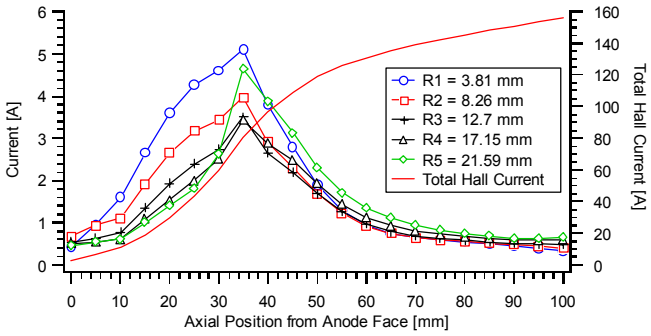

Figure 15, The calculated Hall current radial profiles across the discharge channel and the sum of the profiles as a function of axial position (note that the thruster exit is at 38 mm).

The self-field modeling results for the 300 V 5.4 A thruster discharge condition is presented in Fig. 16.

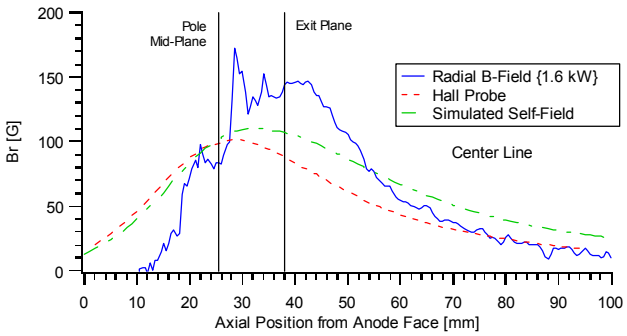

Figure 16, The simulated self-field for the P5 operating at 1.6 kW.

As it can be seen in Fig. 16, the model predicts a change in the radial magnetic field profile along the center of the discharge channel. Similar results are obtained for the 300 V and 10 A thruster condition (not shown). However, these observed changes are not as large as the measured field profiles from the B-Dot probe. This could possibly be due to the technique used to calculate the Hall current from the Hall parameters or a problem with the calculated Hall parameters.

Another issue that has not been discussed in this paper is the possibility of a dielectric sheath forming around the probe [24,25]. Since the probe is constructed of a dielectric material and is inserted into the discharge plasma of the thruster, the azimuthal electron current would dominate the collisions with the probe's surface thus establishing a negative sheath that might redirect the Hall current around the probe. This could increase the electron current density to ether side of the probe, thereby changing the normal Hall current profile. The dielectric sheath thickness is on the order of Debye length (λ_D) [25], which is expressed as follows.

$$\lambda_D = \sqrt{\frac{kT_e}{4\pi e^2 n_e}} \qquad (5)$$

The sheath thickness was determined from eq. (5) to be approximately 0.05 mm for the internal plasma parameters of the P5 thruster operating a 1.6 kW [5]. The sheath thickness is not large compared to the size of the probe, but the probe and the thin sheath could effect the profile of the Hall current. A Magnet model was devised that would test the possibility of the modified Hall current. The results from the model, not shown, did indicate a change in the self-field radial magnetic field profile as seen in Fig. 16. The other issue with a dielectric probe is that it could be absorbing high-energy electrons and re-emitting probe temperature electrons. This thermalization of the Hall current would reduce the overall Hall current for the system, thereby reducing the Hall current self-field.

The predicted thrust, for a Hall thruster, can be obtained analytically from the magnetohydrodynamic (MHD) momentum equation [5] shown in eq. (6) and knowing the azimuthal Hall current (j_{Hall}) in a given volume (V) and the radial magnetic field (B_r).

$$\mathbf{F} = -\nabla P + \rho_c \mathbf{E} + \mathbf{j}x\mathbf{B} \qquad (6)$$

Assuming that the electron pressure term (∇P) is small and a quasineutral plasma (ρ_c=0), eq. (6) reduces to the following **j**x**B** force.

$$F_y(r,z) = j_{Hall}(r,z) B_r(r,z) V(r,z) \qquad (7)$$

Equation (7) can be used to calculate the thrust in each individual Hall current region, as described above, then the total thruster can be found by summing all the regions. The measured thrust for the P5 at the 1.6 kW condition referred to in this paper was 98 mN [20]. The calculated thrust for the Hall current shown in Fig. 15 using eq. (7) and the measured radial magnetic field profiles from the B-Dot probe at the 1.6 kW plasma case was approximately 300 mN. This calculated thrust is much greater than the measured 98 mN. The calculated Hall current from the measured electric field and the vacuum magnetic field in reference [5] and the radial vacuum magnetic fields indicate a thrust of 105 mN. The results for this case are within good agreement with measured thrust for the P5. The conclusion of this exercise is that a Hall current significantly large enough to produce the self-field observed in the B-Dot probe traces would equate to a thrust much larger than what is experimental measured at the operating point of 300 V and 5.4 A.

It was shown in magnetic field integration impact testing [26] of the D-55, anode lever thruster, that a 22% increase in the magnetic dipole at 1.28 m behind thruster exit plane was observed between the vacuum applied field and the measured magnetic dipole during 300 V and 2.5 A thruster operation. The data presented in the D-55 paper indicates a significant change in the magnetic field of the thruster during operation. The authors concluded that the change in the axial magnetic field was due to the discharge current passing between the anode and the cathode, thruster body. However, the current passing the discharge is on the order of a few amps and flowing in the wrong direction to provide the results measured with the three-axis fluxgate magnetometer. To obtain the change in the axial magnetic field observed during the test a loop of current, with its axis passing through the point of investigation (1.28 m behind the thruster), on the order of 50 A is needed. The current required to justify the 22% change was determined from the definition of a magnetic dipole moment.

$$\mu = NIA_{loop} \qquad (8)$$

The magnetic dipole is a product of the number of turns in the loop (N), the current passing through each turn (I), and the area of the loop (A_{loop}). For this calculation the number of turns was assumed to be one with a loop area determined from the mean diameter of the D-55 thruster anode plus an assumption of 20 mm to account for the width of the Hall Current. A

region of Hall current, on the order of 50 A, adjacent to anode would possible explain the measured magnetic dipole moment reported in D-55 paper [26]. A Hall current of this magnitude would result in a Hall to discharge current ratio of approximately 24 and thus a Hall parameter roughly of 515, assuming a Hall current cross-section 4 cm^2. Repeating the thrust calculation for the D-55, as described previously, and assuming an average radial magnetic field of 100 G the calculated thrust is 86 mN. The measured thrust of the D-55 (RHETT2/EPDM) was 43.2 mN [27].

Conclusions

The magnetic field topography of the P5 Hall thruster was successfully mapped during operation of the thruster with a plasma discharge. The experimentally mapped magnetic field profiles along the width of the discharge channel of a Hall thruster deviated from the vacuum field profile, as measured with a Hall probe. The largest increase observed was approximately 70 G on the centerline sweep of the 1.6 kW operation condition. These results were accomplished by the development of a new PEPL HARP system internal plasma diagnostic technique with the incorporation of a B-Dot probe. The Hall current of the P5 was then calculated from a previously determined Hall parameter and incorporated into a 3D magnetostatic model to determine if there was any possible influence on the applied magnetic field topography from the calculated Hall current. The **j**x**B** forces were then solved to establish if the Hall current required to influence the magnetic field topography, as observed in the B-Dot probe measurements, is probable. The calculated thrust values from the **j**x**B** force were 2 to 3 times the actual measured values at the given operating parameters. Several experiments and calculations were conducted to test the B-Dot probe system reliability under the plasma conditions of a typical Hall thruster discharge. The experiments and calculations did not demonstrate any conclusive evidence of a flaw in the design or methodology utilized for measuring the magnetic field discussed in this paper. Furthermore, the topic is complicated by documentation of independent non-intrusive magnetic dipole measurements of the D-55 at NASA Glenn Research Center. The magnetic dipole measurements of the D-55 just suggest a 22% increase of the measured magnetic dipole with and without a plasma discharge. It is clear that a better understanding of the influence of a Hall thruster self-field is required if higher power thrusters are to be realized.

Acknowledgements

The authors would like to acknowledge the support of this research by NASA through contract NGT3-52348 and NAG3-2307 (Robert Jankovsky, technical monitor for both grants). The authors would also like to thank the Air Force Research Laboratory for their assistance in the design and fabrication of the P5 Hall thruster, Dr. Sergi Khartov at MAI for the use of the LaB_6 cathode, and the graduate students at PEPL for their assistance in setting up and running the experiments for this investigation. The authors would also like to thank the technical support staff of the Aerospace Engineering Department.

References

1. Butler, G.W., Yuen, J.L., Tverdokhlebov, S.O., Semenkin, A.V., Kochergin, A.V., Solodulthin, A.E., Jankovsky, R.S., "Multimode, High Specific Impulse Hall Thruster Technology," AIAA-00-3254, 36th Joint Propulsion Conference (JPC) Huntsville, AL, July 16-19, 2000.

2. Oleson, S. R., "Mission Advantages of Constant Power, Variable Isp Electrostatic Thrusters," AIAA-00-3413, 36th Joint Propulsion Conference (JPC) Huntsville, AL, July 16-19, 2000.

3. Gavryshin, et al., "Physical and Technical Bases of the Modern SPT Development," IEPC-95-38

4. Kim, V., "Main Physical Features and Process Determining the Performance of Stationary Plasma Thrusters", Journal of Propulsion and Power, Vol. 14, No. 5, September-October 1998

5. Haas, J.M., "Low-perturbation Interrogation of the Internal and Near-field Plasma Structure of a Hall Thruster Using a High-Speed Probe Positioning System," Ph.D. Dissertation, University of Michigan, 2001.

6. Meezan, N.B., Cappelli, M.A., "Electron density measurements for determining the anomalous electron mobility in coaxial discharge plasma," AIAA-00-3420, 36th Joint Propulsion Conference (JPC) Huntsville, AL, July 16-19, 2000

7. Haas, J.M., Gallimore, A.D., McFall, K., and Spanjers, G., "Development of a High-Speed, Reciprocating Electrostatic Probe System for Hall Thruster Interrogation," Review of Scientific Instruments, Vol. 71, No. 11, pp. 4131-4138, November 2000.

8. Williams, G., Smith, T., Gallimore, A.D., "FMT-2 Discharge Cathode Erosion Rate Measurements via Laser Induced Fluorescence," AIAA-00-3663, 36th Joint Propulsion Conference (JPC) Huntsville, AL, July 16-19, 2000.

9. Beal, B.E., Haas, J.M., Gallimore, A.D., "Plasma Density Measurements Inside a Laboratory Model Hall Thruster Using a Resonance Probe Diagnostic," ICOPS-00-4A03, 27th IEEE International Conference on Plasma Science (ICOPS) New Orleans, LA June 4-7, 2000.

10. Hofer, R.R., Haas, J.M., and Gallimore, A.D., "Development of a 45-Degree Parallel-Plate Electrostatic Energy Analyzer for Hall Thruster Plume Studies: Preliminary Data," IEPC-99-113, 26th International Electric Propulsion Conference, Kitakyushu, Japan, October 1999.

11. Gulczinksi, F.S., Hofer, R.R., and Gallimore A.D., "Near-field Ion Energy and Species Measurements of a 5 kW Laboratory Hall Thruster, " AIAA-99-2430, 35th Joint Propulsion Conference, Los Angeles, CA, June 1999.

12. Kim, S., and Gallimore, A.D., "Plume Study of a 1.35 kW SPT-100 Using an ExB Probe, " AIAA-99-2423, 35th Joint Propulsion Conference, Los Angeles, CA, June 1999.

13. King, L. B., and Gallimore, A. D., "A Gridded Retarding Pressure Sensor for Ion and Neutral Particle Analysis in Flowing Plasmas," Review of Scientific Instruments, Vol. 68, No. 2, Feb. 1997, 1183-1188.

14. Domonkos, M. T., Gallimore, A. D., Marrese, C. M., and Haas, J. M., "Very Near-Field Plume Investigation of the Anode Layer Thruster," Journal of Propulsion and Power (AIAA), Vol. 16, No. 1, January-February 2000.

15. Lovberg, R. H., "Plasma Diagnostic Techniques," Chapter 3, Academic Press Inc., 1965.

16. Piejak, R., Godyak, V., Alexandrovich, B., "The electric field and current density in a low-pressure inductive discharge measure with B-Dot probes," Journal of Applied Physics, American Institute of Physics, Vol. 81, No. 8, April 1997.

17. Black, D.C., "Direct Magnetic Field Measurements of Flow Dynamics and Micro-Turbulence Enhanced Electron Collisionality in Magnetized Coaxial Accelerator Channels," Ph.D. Dissertation, North Carolina State University, 1996.

18. Barkalov, E.E., Veselovzorov, A.N, Subbotin, M.L., "Experimental study of the azimuthal electron drift current in Hall accelerators," Sov. Phys. Tech. Phys., Vol. 35, No. 2, February 1990

19. Haas, J.M., and Gallimore, A.D., "Characterization of the Internal Plasma Structure of a 5 kW Hall Thruster," IEPC-99-078, 26th International Electric Propulsion Conference, Kitakyushu, Japan, October 1999.

20. Haas, J. M., Gulczinski, F. S., Gallimore, A. D., Spanjers, G.G., Spores, R.A., "Performance Characteristics of a 5 kW Laboratory Hall Thruster," AIAA-98-3503, 34th Joint Propulsion Cleveland, OH, July 12-15, 1998.

21. Hofer, R.R., Jankovsky, R.S., "A Hall Thruster Performance Model Incorporating the Effects of a Multiply-Charged Plasma," AIAA-01-3322, 37th Joint Propulsion Salt Lake City, Utah, July 8-11, 2001.

22. Hofer, R. R., Peterson, P. Y., Gallimore, A. D., "A High Specific Impulse Two-Stage Hall Thruster with Plasma Lens Focusing," IEPC-01-036, 27th International Electric Propulsion Conference, Pasadena, CA, Oct 14-19, 2001.

23. Williams, G.J., Smith, T.B., Gulczinski, F.S., Beal, B.E., Gallimore, A.D., and Drake, R.P., "Laser Induced Fluorescence Measurement of Ion Velocities in the Plume of a Hall Effect Thruster," AIAA-99-2424, 35th Joint Propulsion Conference, Los Angeles, CA, June 1999.

24. Ahedo, E., Martínez Cerezo, P., Martínez-Sánchez, M., "Model of Plasma-Wall Interaction Effects in a Hall Thruster," AIAA-01-3323, 37th Joint Propulsion Salt Lake City, Utah, July 8-11, 2001.

25. UHM, H. S., "Reduction of sheath electric field by multidielectric slabs in a plasma," J. Plasma Physics (2000), vol. 63, part 2, pp. 129-137.

26. Sankovic, J.M., Pencil, E.J., Jacobson, D.T., "RHETT2/EPDM Magnetic Field Integration Impacts," IEPC-97-109, 25th International Electric Propulsion Conference, Cleveland, OH, Aug 24-28, 1997.

27. Sankovic, J.M., Manzella, D.H., Osborn, M.F., "RHETT2/EPDM Development Testing," IEPC-97-102, 25th International Electric Propulsion Conference, Cleveland, OH, Aug 24-28, 1997.